

# Electronic Supplementary Information (ESI)

## Detection of persistent organic pollutants of polychlorinated benzenes by a lanthanide metal-organic framework luminescent sensor

Lu Wang,<sup>a</sup> Guilan Fan,<sup>a</sup> Xiufang Xu,<sup>a</sup> Diming Chen,<sup>a</sup> Liang Wang,<sup>\*b</sup> Wei Shi<sup>\*acd</sup> and Peng Cheng<sup>\*acd</sup>

<sup>a</sup>Department of Chemistry, Key Laboratory of Advanced Energy Materials Chemistry(MOE), Nankai University, Tianjin 300071, China. E-mail: shiwei@nankai.edu.cn; pcheng@nankai.edu.cn

<sup>b</sup>State Key Laboratory of Separation Membranes and Membrane Processes, Tianjin Polytechnic University, Tianjin 300387, China

<sup>c</sup>State Key Laboratory of Elemento-Organic Chemistry, Nankai University, Tianjin 300071, China

<sup>d</sup>Collaborative Innovation Center of Chemical Science and Engineering (Tianjin), Nankai University, Tianjin 300071, China

### *Contents of ESI*

<b>Table S1</b>	Crystal Data and Structural Refinement Parameters for Ln-MOF 1.	p.3
<b>Table S2</b>	Selected bond lengths (Å) and angles (°) for Ln-MOF 1.	p.4
<b>Fig. S1</b>	Simulated and experimental powder X-ray diffraction patterns of Ln-MOF 1.	p.4
<b>Fig. S2</b>	Fourier transform infrared (FT-IR) spectrum of Ln-MOF 1.	p.5
<b>Fig. S3</b>	Simplified topological structure of Ln-MOF 1.	p.5
<b>Fig. S4</b>	Thermal gravimetric analyses (TGA) curve of Ln-MOF 1.	p.6
<b>Fig. S5</b>	The solid-state excitation and emission spectra with the excitation wavelength of 294 nm of Ln-MOF 1 at room temperature. Insert: the colors of Ln-MOF 1 before (above) and after (below) the irradiation of UV light of 254 nm.	p.6
<b>Fig. S6</b>	The solid-state excitation and emission spectra of H <sub>2</sub> L at room	p.7

temperature.

- Fig. S7** Powder X-ray diffraction patterns of Ln-MOF **1** after dissolved in different organic solvents. p.7
- Fig. S8** Luminescence quenching ( $I/I_0$ ) of Ln-MOF **1** (3 mg) dispersed in 3mL DMF with different organic solvents added when excited at 294 nm. p.8
- Fig. S9** (a) Suspension-state PL spectra and (b) the  $^5D_0 \rightarrow ^7F_2$  transition intensities of Ln-MOF **1** with different addition of chlorobenzene when excited at 294 nm. p.8
- Fig. S10** (a) Suspension-state PL spectra and (b) the  $^5D_0 \rightarrow ^7F_2$  transition intensities of Ln-MOF **1** with different addition of 1,4-dichlorobenzene when excited at 294 nm. p.9
- Fig. S11** (a) Suspension-state PL spectra and (b) the  $^5D_0 \rightarrow ^7F_2$  transition intensities of Ln-MOF **1** with different addition of 1,2,4-TCB when excited at 294 nm. p.9
- Fig. S12** (a) Suspension-state PL spectra and (b) the  $^5D_0 \rightarrow ^7F_2$  transition intensities of Ln-MOF **1** with different addition of 1,2,3,4-TCB when excited at 294 nm. p.9
- Fig. S13** (a) Suspension-state PL spectra and (b) the  $^5D_0 \rightarrow ^7F_2$  transition intensities of Ln-MOF **1** with different addition of 1,2,4,5-TCB when excited at 294 nm. p.10
- Fig. S14** (a) Suspension-state PL spectra and (b) the  $^5D_0 \rightarrow ^7F_2$  transition intensities of Ln-MOF **1** with different addition of PeCB when excited at 294 nm. p.10
- Fig. S15** (a) Suspension-state PL spectra and (b) the  $^5D_0 \rightarrow ^7F_2$  transition intensities of Ln-MOF **1** with different addition of HCB when excited at 294 nm. p.10

<b>Fig. S16</b>	Reproducibility of the quenching ability of Ln-MOF <b>1</b> for 1,2,4-TCB with five continuous quenching cycles.	p.11
<b>Fig. S17</b>	Molecular structures and sizes of polychlorinated benzenes.	p.11
<b>Fig. S18</b>	HOMO and LUMO energies calculated for ligand H <sub>2</sub> L and polychlorinated benzenes.	p.12
<b>Fig. S19</b>	The UV-vis absorption spectra for chlorobenzene, 1,2-dichlorobenzene, 1,2,4-TCB (a), 1,2,3,4-TCB, 1,2,4,5-TCB, PeCB, HCB and H <sub>2</sub> L (c); comparison of PL spectra of Ln-MOF <b>1</b> before and after adding 1,2,4-TCB (1.25%) (b), 1,2,3,4-TCB, 1,2,4,5-TCB, PeCB, HCB (4.00 mM) (d).	p.12
<b>Tables S3–S9</b>	The Cartesian Coordinates of the stationary points discussed in this paper.	p.13-17

**Table S1.** Crystal data and structural refinement parameters for Ln-MOF **1**.

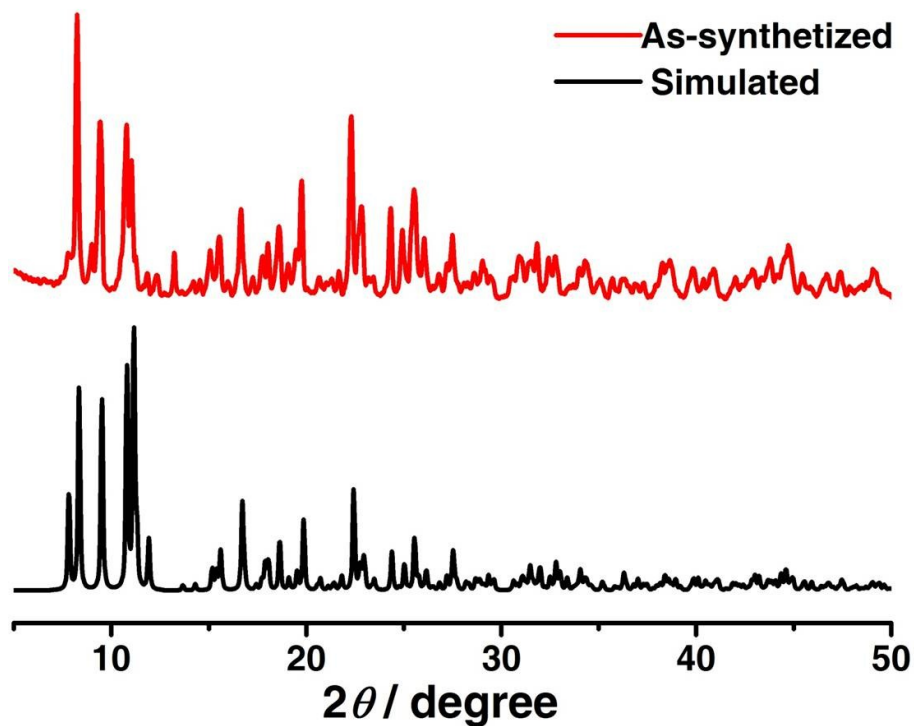
<b>1</b>	
Formula	C <sub>40</sub> H <sub>40</sub> N <sub>12</sub> O <sub>16</sub> Eu <sub>2</sub>
F.M	1248.74
T /K	122
Crystal system	Monoclinic
Space group	<i>I</i> 2/ <i>a</i>
<i>a</i> / Å	17.4164(6)
<i>b</i> / Å	14.2453(4)
<i>c</i> / Å	20.4424(7)
$\alpha$ /°	90.00
$\beta$ /°	114.512(4)
$\gamma$ /°	90.00
V/ Å <sup>3</sup>	4614.7(3)
<i>Z</i>	4
$\mu$ /mm <sup>-1</sup>	2.765
Reflns collected	9331
Independ. reflns	4063
<i>R</i> <sub>int</sub>	0.0389
<i>R</i> <sub>1</sub> <sup>a</sup> ( <i>I</i> > 2σ( <i>I</i> ))	0.0282
<i>wR</i> <sub>2</sub> <sup>a</sup> (all data)	0.0536
GOF	1.002

$${}^a R_1 = \frac{\sum ||F_0| - |Fc||}{\sum |F_0|}, \quad {}^b wR_2 = \left[ \frac{\sum w(F_0^2 - F_c^2)^2}{\sum w(F_0^2)^2} \right]^{1/2}.$$



**Table S2.** Selected bond lengths (Å) and angles (°) for Ln-MOF **1**.

<b>1</b>					
Eu1-O6	2.387(5)	O6-Eu1-N7	73.49(16)	O12-Eu1-O9	107.33(16)
Eu1-N7	2.581(5)	O6-Eu1-O8	133.25(16)	O22-Eu1-O6	124.08(17)
Eu1-O8	2.474(4)	O6-Eu1-O9	82.70(16)	O22-Eu1-N7	148.39(18)
Eu1-O9	2.501(4)	O6-Eu1-O11	77.66(16)	O22-Eu1-O8	86.50(16)
Eu1-O11	2.401(4)	O6-Eu1-O12	141.47(18)	O22-Eu1-O9	133.29(16)
Eu1-O12	2.404(5)	O8-Eu1-N7	99.08(16)	O22-Eu1-O11	78.64(16)
Eu1-O22	2.297(5)	O8-Eu1-O9	52.62(15)	O22-Eu1-O12	76.24(19)
Eu1-O26	2.333(4)	O9-Eu1-N7	69.69(15)	O22-Eu1-O26	74.9(2)
		O11-Eu1-N7	80.61(15)	O26-Eu1-O6	78.75(19)
		O11-Eu1-O8	148.06(15)	O26-Eu1-N7	136.76(19)
		O11-Eu1-O9	148.04(15)	O26-Eu1-O8	76.76(16)
		O11-Eu1-O12	75.15(16)	O26-Eu1-O9	74.49(17)
		O12-Eu1-N7	75.55(17)	O26-Eu1-O11	124.88(17)
		O12-Eu1-O8	73.91(16)	O26-Eu1-O12	139.63(19)

**Fig. S1** Simulated and experimental powder X-ray diffraction patterns of Ln-MOF **1**.

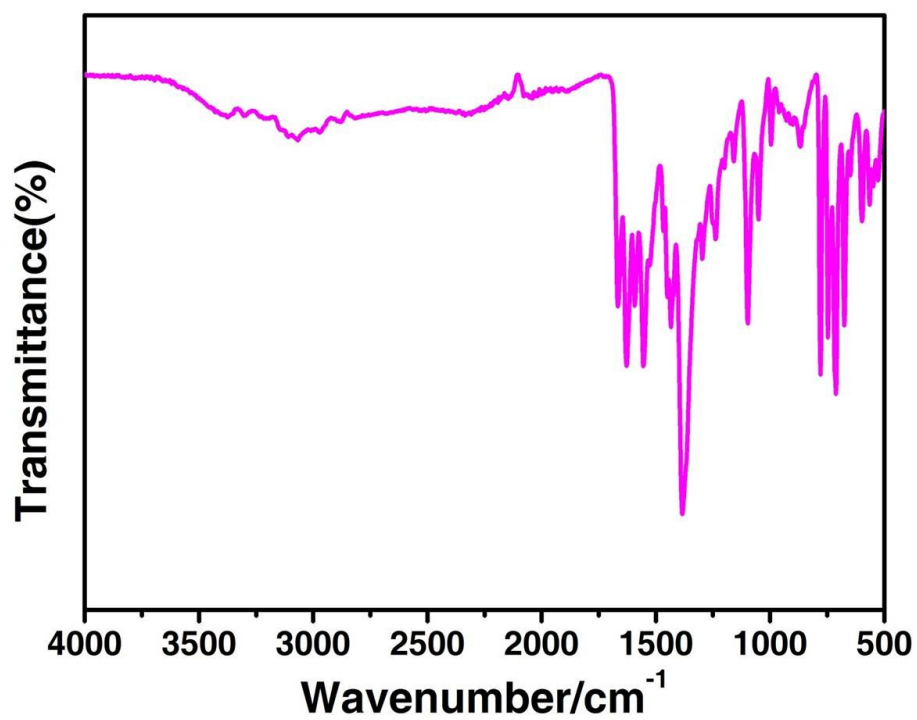


**Fig. S2** Fourier transform infrared (FT-IR) spectrum of Ln-MOF **1**.

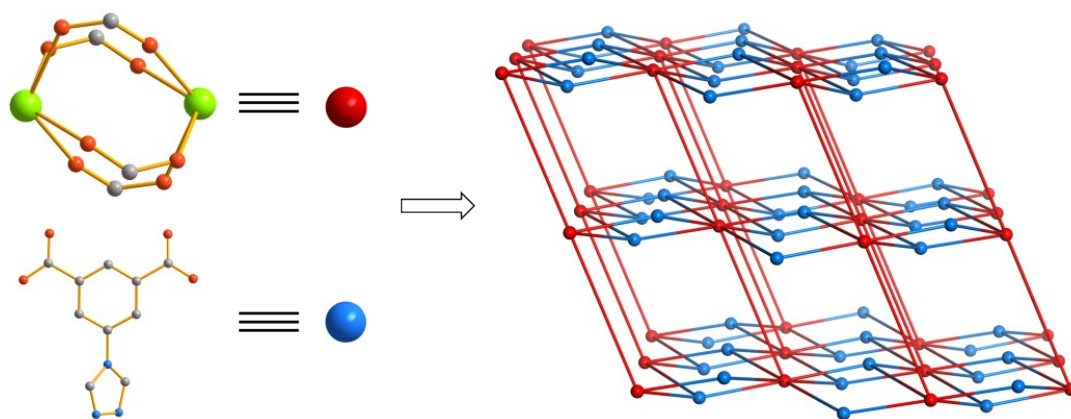


**Fig. S3** Simplified topological structure of Ln-MOF **1**: (red)  $\text{Ln}_2$  binuclear unit; (blue)  $\text{L}^2$  ligand.

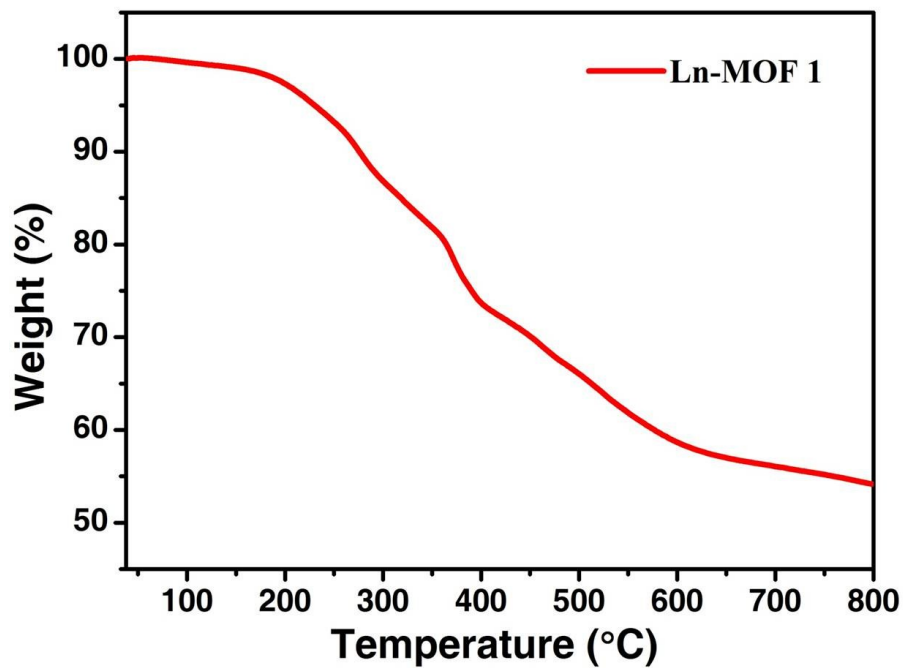


Fig. S4 Thermal gravimetric analyses (TGA) curve of Ln-MOF 1.

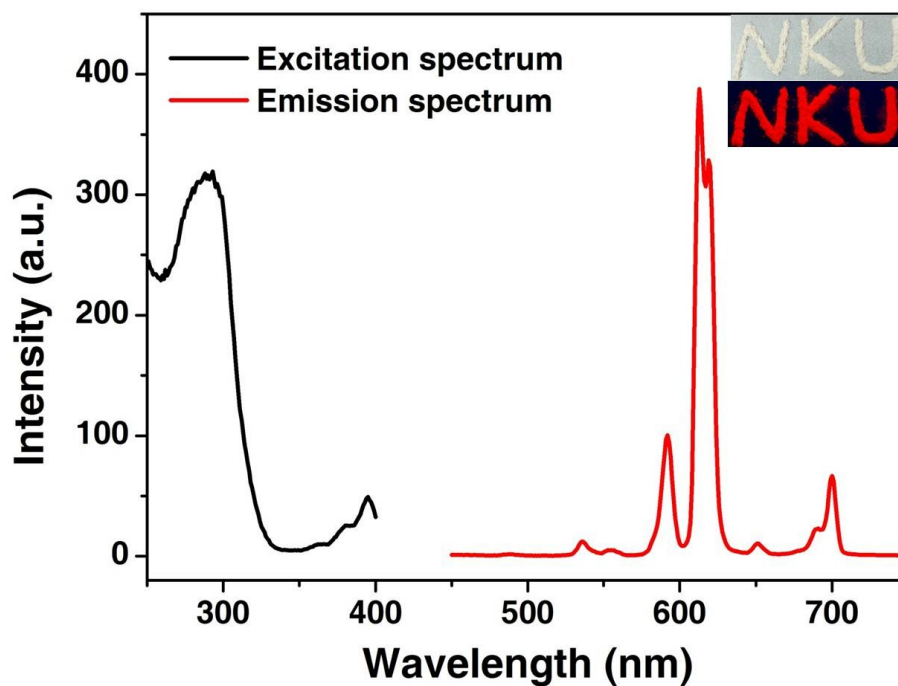
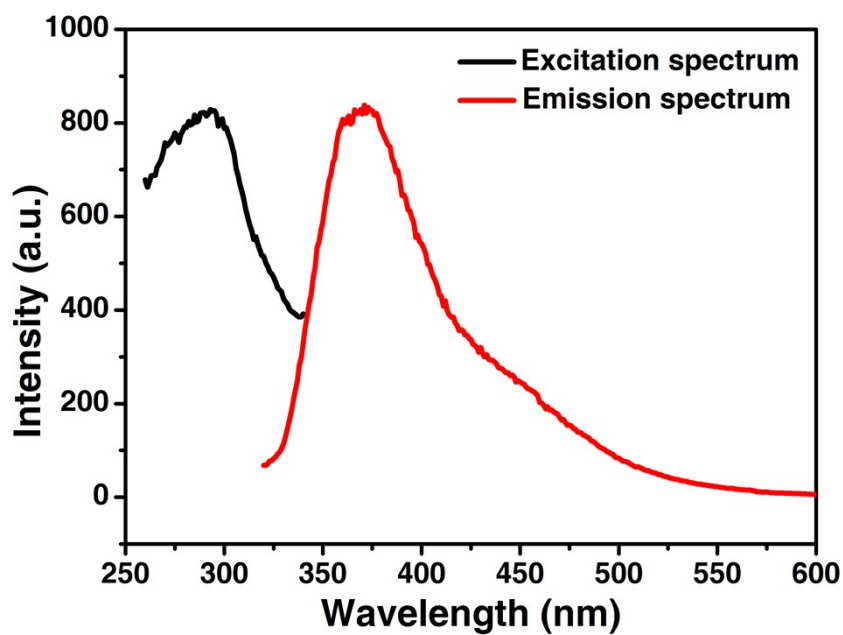
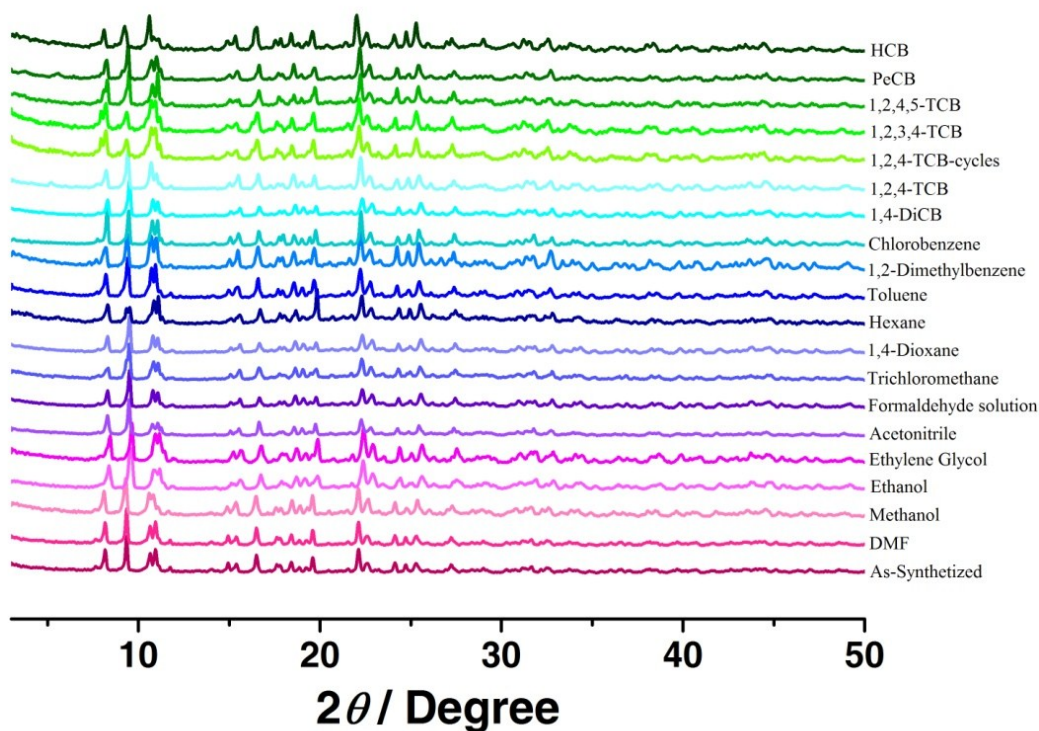


Fig. S5 The solid-state excitation and emission spectra with the excitation wavelength of 294 nm of Ln-MOF 1 at room temperature. Insert: the colors of Ln-MOF 1 before (above) and after (below) the irradiation of UV light of 254 nm.



**Fig. S6** The solid-state excitation and emission spectra of H<sub>2</sub>L at room temperature.



**Fig. S7** Powder X-ray diffraction patterns of Ln-MOF 1 after immersing in different organic solvents.



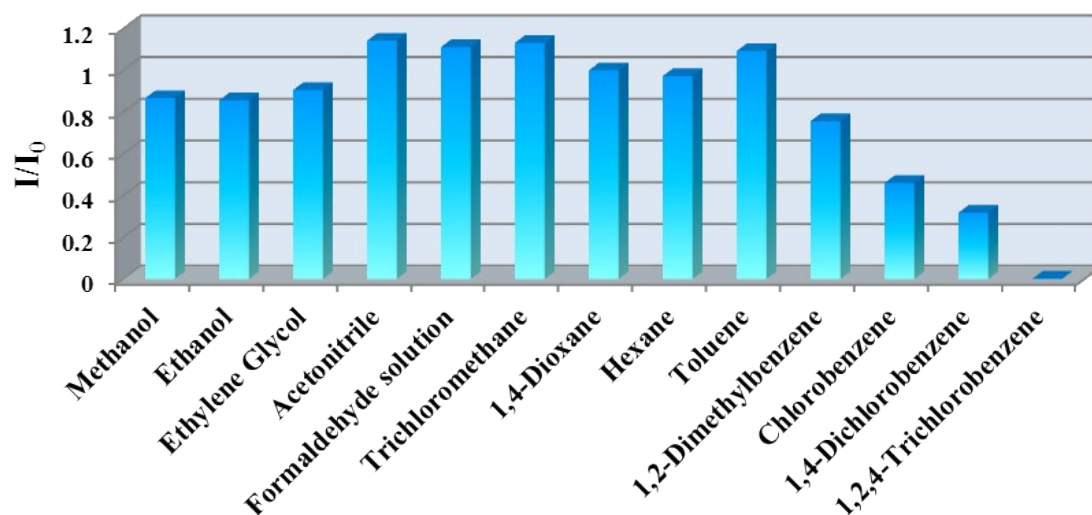


**Fig. S8** Luminescence quenching ( $I/I_0$ ) of Ln-MOF **1** (3 mg) dispersed in 3 mL DMF with different organic solvents added when excited at 294 nm.

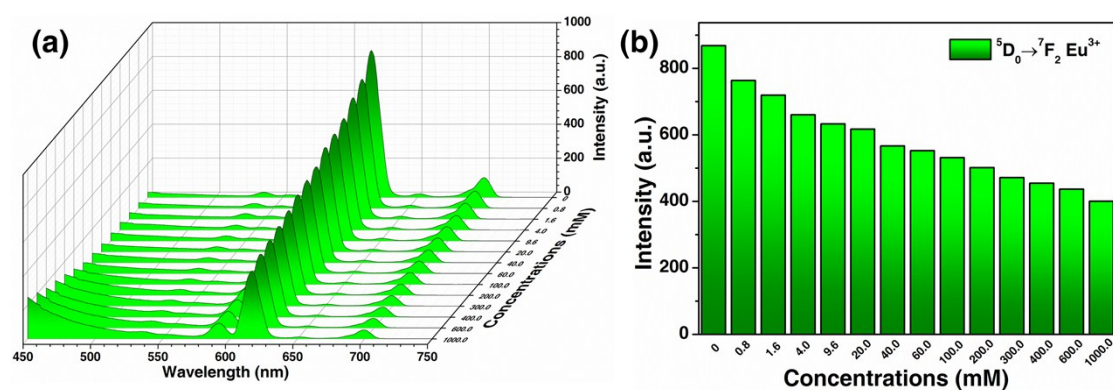


**Fig. S9** (a) Suspension-state PL spectra and (b) the  $^5D_0 \rightarrow ^7F_2$  transition intensities of Ln-MOF **1** with different addition of chlorobenzene when excited at 294 nm.

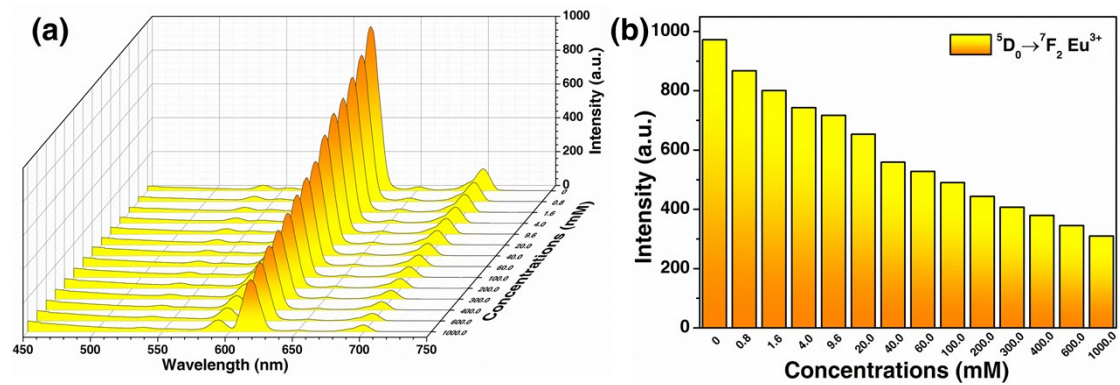


**Fig. S10** (a) Suspension-state PL spectra and (b) the  $^5D_0 \rightarrow ^7F_2$  transition intensities of Ln-MOF **1** with different addition of 1,4-dichlorobenzene when excited at 294 nm.

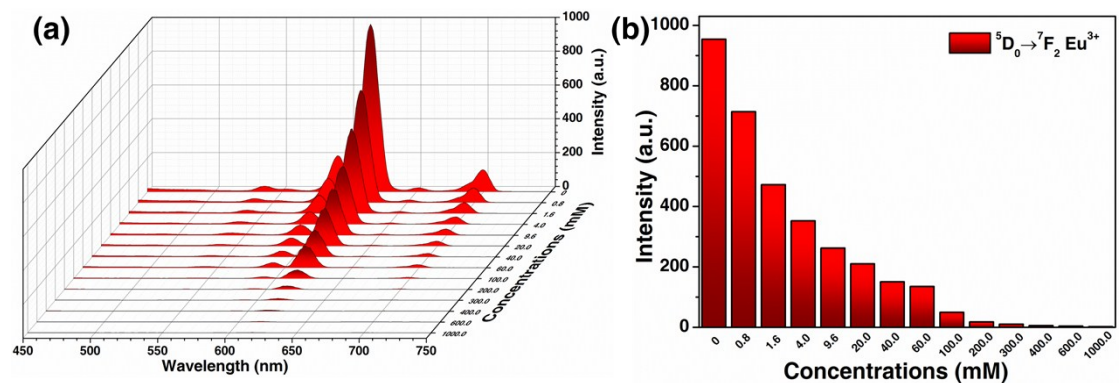


**Fig. S11** (a) Suspension-state PL spectra and (b) the  $^5D_0 \rightarrow ^7F_2$  transition intensities of Ln-MOF **1** with different addition of 1,2,4-TCB when excited at 294 nm.

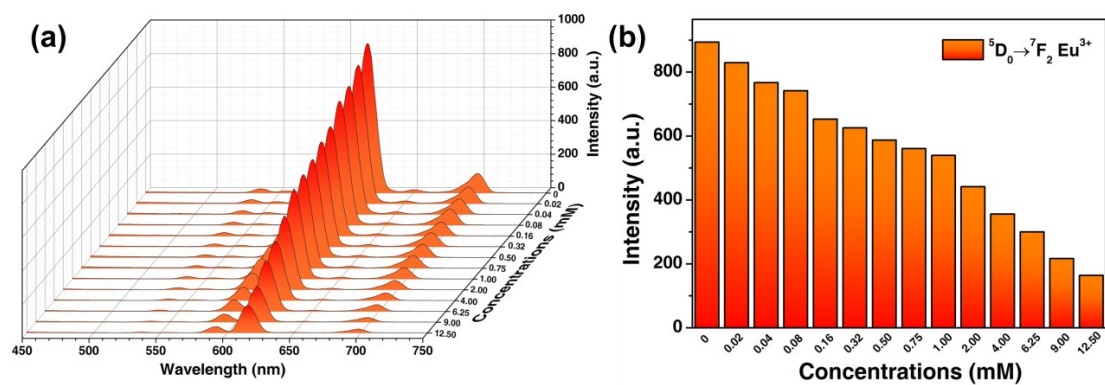


**Fig. S12** (a) Suspension-state PL spectra and (b) the  $^5D_0 \rightarrow ^7F_2$  transition intensities of Ln-MOF **1** with different addition of 1,2,3,4-TCB when excited at 294 nm.

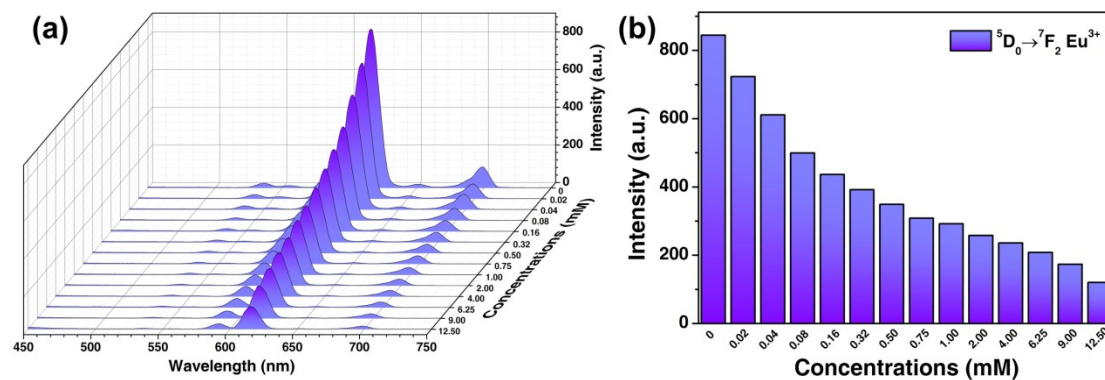


**Fig. S13** (a) Suspension-state PL spectra and (b) the  $^5D_0 \rightarrow ^7F_2$  transition intensities of Ln-MOF **1** with different addition of 1,2,4,5-TCB when excited at 294 nm.

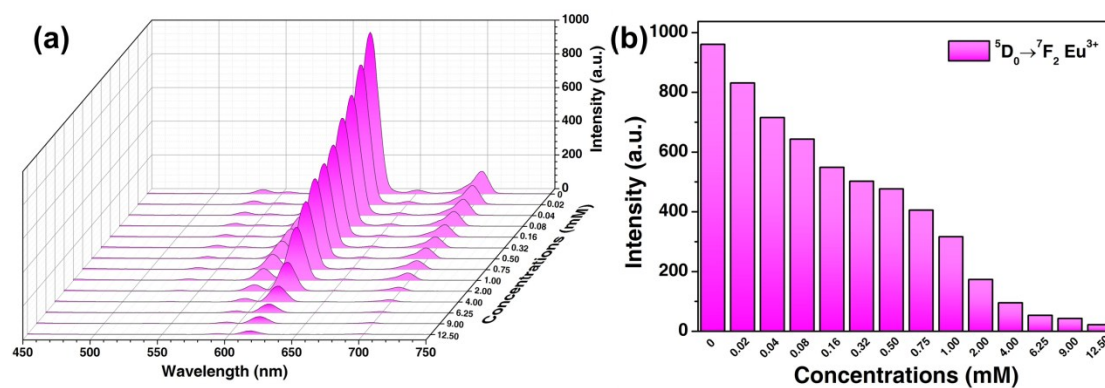


**Fig. S14** (a) Suspension-state PL spectra and (b) the  $^5D_0 \rightarrow ^7F_2$  transition intensities of Ln-MOF **1** with different addition of PeCB when excited at 294 nm.

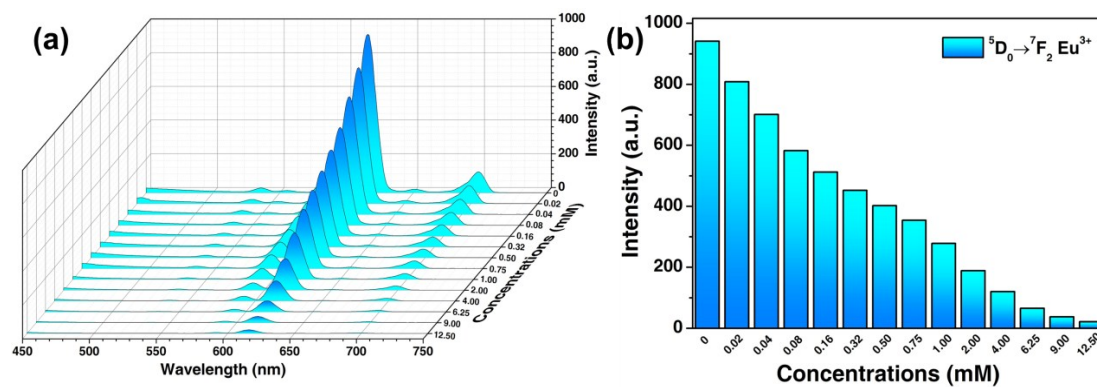


**Fig. S15** (a) Suspension-state PL spectra and (b) the  $^5D_0 \rightarrow ^7F_2$  transition intensities of Ln-MOF 1 with different addition of HCB when excited at 294 nm.

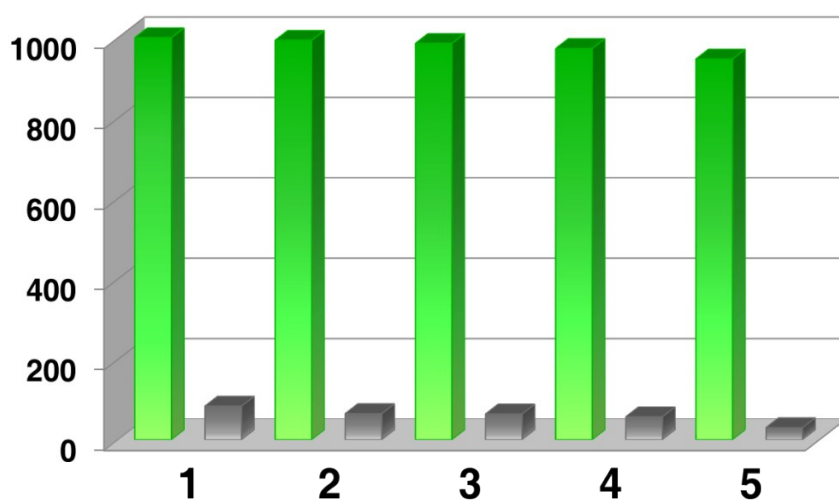


**Fig. S16** Reproducibility of the quenching ability of Ln-MOF 1 for 1,2,4-TCB with five continuous quenching cycles.

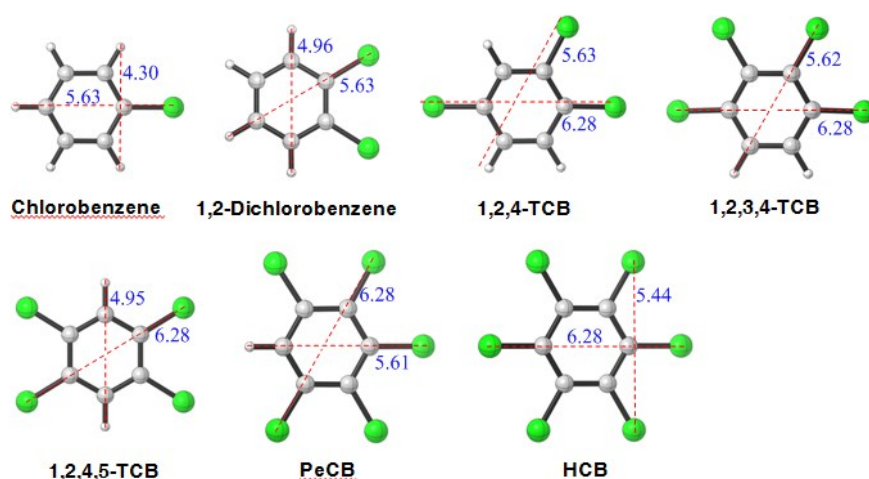


Fig. S17 Molecular structures and sizes of polychlorinated benzenes.

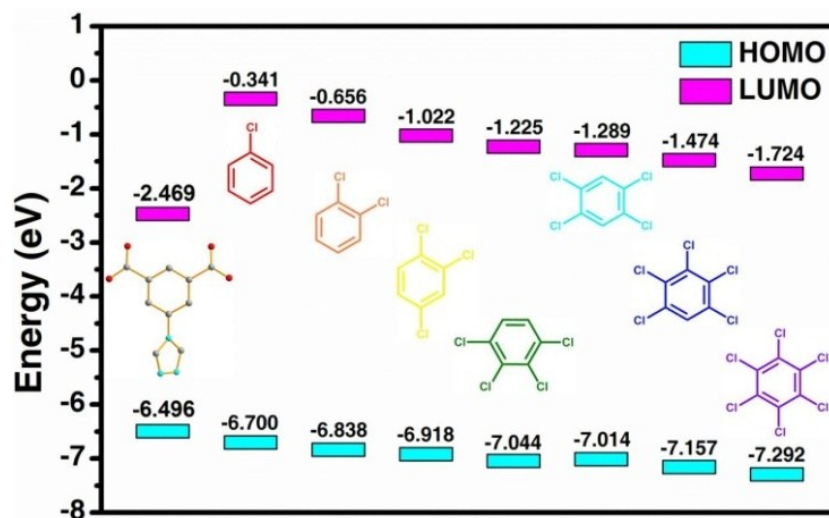


Fig. S18 HOMO and LUMO energies calculated for ligand H<sub>2</sub>L and polychlorinated benzenes.

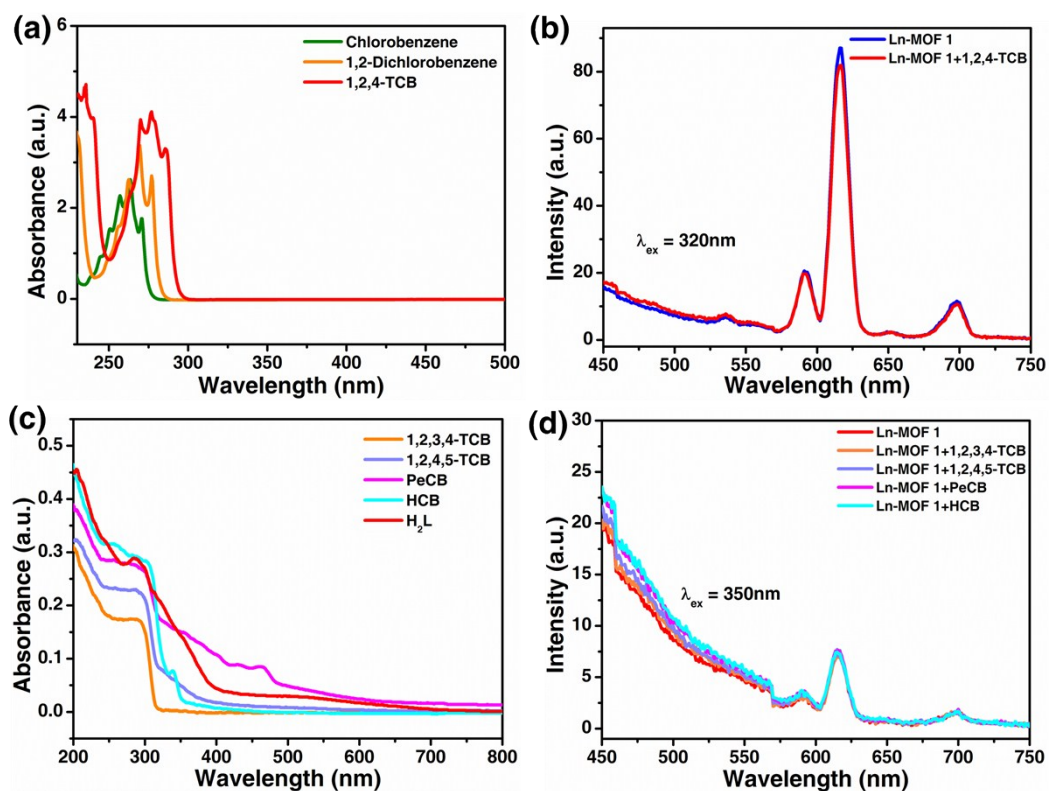


Fig. S19 The UV-vis absorption spectra for chlorobenzene, 1,2-dichlorobenzene, 1,2,4-TCB (a), 1,2,3,4-TCB, 1,2,4,5-TCB, PeCB, HCB and H<sub>2</sub>L (c); comparison of

PL spectra of Ln-MOF **1** before and after adding 1,2,4-TCB (1.25%) (b), 1,2,3,4-TCB, 1,2,4,5-TCB, PeCB, HCB (4.00 mM) (d).

### DFT Calculation.

The geometries of all minima were fully optimized in gas phase using the hybrid B3LYP<sup>1</sup> functional. The 6-31G(d) basis set was employed for all atoms except for Eu. The large core ECP52MWB<sup>2</sup> optimized by the Stuttgart/Cologne group was used for uranium centers. Frequency calculations were performed at 298.15 K to verify that the stationary points were the local minima. All of the calculations were performed with Gaussian 09.<sup>3</sup>

**Tables S3–S9.** The Cartesian Coordinates of the stationary points discussed in this paper.

For all minimum structures, no imaginary frequency was observed.

**Table S3. Chlorobenzene**

Atom	X	Y	Z
C	-1.574505	-1.207803	0.000000
C	-0.178309	-1.216394	0.000000
C	0.504285	0.000000	0.000000
C	-0.178309	1.216394	0.000000
C	-1.574505	1.207803	-0.000000
C	-2.275148	0.000000	0.000000
H	-2.112520	-2.151833	-0.000000
H	0.374772	-2.149683	-0.000000
H	0.374772	2.149683	0.000000
H	-2.112520	2.151833	-0.000000
H	-3.361301	0.000000	-0.000000
Cl	2.264455	0.000000	-0.000000

**Table S4. 1,2-Dichlorobenzene**

Atom	X	Y	Z
C	0.000000	2.392333	0.697816
C	-0.000000	1.185558	1.394869
C	0.000000	-0.027127	0.700823
C	0.000000	-0.027127	-0.700823
C	0.000000	1.185558	-1.394869
C	0.000000	2.392333	-0.697816
H	-0.000000	3.328481	1.248168
H	-0.000000	1.169473	2.479526
H	-0.000000	1.169473	-2.479526
H	-0.000000	3.328481	-1.248168
Cl	-0.000000	-1.517796	1.613147
Cl	-0.000000	-1.517796	-1.613147

**Table S5. 1,2,4-TCB**

Atom	X	Y	Z
C	-1.724824	-0.146562	-0.000000
C	-0.811558	0.904996	-0.000000
C	0.557015	0.625186	-0.000000
C	1.003376	-0.703799	-0.000000
C	0.069940	-1.743064	-0.000000
C	-1.296264	-1.473514	-0.000000
H	-1.151513	1.933561	0.000000
H	0.423255	-2.768520	0.000000
H	-2.017019	-2.283389	0.000000
Cl	1.676028	1.963104	0.000000
Cl	2.702985	-1.096880	0.000000
Cl	-3.440239	0.212534	0.000000

**Table S6. 1,2,3,4-TCB**

Atom	X	Y	Z
C	-1.395435	-0.817966	-0.000000
C	-0.704667	0.404342	-0.000000
C	0.704667	0.404342	-0.000000
C	1.395435	-0.817966	-0.000000
C	0.694632	-2.023501	-0.000000
C	-0.694632	-2.023501	-0.000000
H	1.243971	-2.958230	0.000000
Cl	1.577259	1.904245	0.000000
Cl	3.138080	-0.870070	0.000000
Cl	-3.138080	-0.870070	0.000000
H	-1.243971	-2.958230	0.000000
Cl	-1.577259	1.904245	0.000000

**Table S7. 1,2,4,5-TCB**

Atom	X	Y	Z
C	1.211775	-0.700870	-0.000000
C	0.000000	-1.391210	-0.000000
C	-1.211775	-0.700870	-0.000000
C	-1.211775	0.700870	-0.000000
C	-0.000000	1.391210	-0.000000
C	1.211775	0.700870	-0.000000
H	0.000000	-2.474552	0.000000
H	-0.000000	2.474552	0.000000
Cl	-2.693739	-1.616140	0.000000
Cl	-2.693739	1.616140	0.000000
Cl	2.693739	-1.616140	0.000000
Cl	2.693739	1.616140	0.000000



**Table S8. PeCB**

Atom	X	Y	Z
C	-1.206324	-1.100770	-0.000000
C	-1.222307	0.302216	-0.000000
C	0.000000	1.000312	-0.000000
C	1.222307	0.302216	-0.000000
C	1.206324	-1.100770	-0.000000
C	0.000000	-1.794747	-0.000000
Cl	0.000000	2.734474	0.000000
Cl	2.727550	1.162537	0.000000
Cl	-2.683187	-2.023102	0.000000
H	0.000000	-2.877608	-0.000000
Cl	-2.727550	1.162537	0.000000
Cl	2.683187	-2.023102	0.000000

**Table S9. HCB**

Atom	X	Y	Z
C	1.403655	-0.054786	0.000000
C	0.654528	-1.243185	0.000001
C	-0.749261	-1.188303	0.000001
C	-1.403655	0.054786	0.000001
C	-0.654528	1.243185	-0.000000
C	0.749261	1.188303	-0.000000
Cl	-1.674228	-2.654387	0.000001
Cl	-3.135747	0.121849	-0.000001
Cl	3.135747	-0.121849	0.000001
Cl	1.462601	-2.777156	-0.000001
Cl	-1.462601	2.777156	0.000001
Cl	1.674228	2.654387	-0.000001

**References**

1. (a) A. D. Becke, *Phys. Rev. A.*, 1988, **38**, 3098; (b) C. Lee, W. Yang, R. G. Parr,

- Phys. Rev. B.*, 1988, **37**, 785; (c) A. D. Becke, *J. Chem. Phys.*, 1993, **98**, 5648; (d) A. D. Becke, *J. Chem. Phys.*, 1993, **98**, 1372; (e) P. J. Stephens, F. J. Devlin, M. J. Frisch, C. F. Chabalowski, *J. Phys. Chem.*, 1994, **98**, 11623.
2. (a) M. Dolg, H. Stoll, A. Savin, H. Preuss, *Theor. Chim. Acta*, 1989, **75**, 173; (b) M. Dolg, H. Stoll, H. Preuss, *Theor. Chim. Acta*, 1993, **85**, 441.
  3. M. J. Frisch, G. W. Trucks, H. B. Schlegel, G. E. Scuseria, M. A. Robb, J. R. Cheeseman, G. Scalmani, V. Barone, B. Mennucci, G. A. Petersson, H. Nakatsuji, M. Caricato, X. Li, H. P. Hratchian, A. F. Izmaylov, J. Bloino, G. Zheng, J. L. Sonnenberg, M. Hada, M. Ehara, K. Toyota, R. Fukuda, J. Hasegawa, M. Ishida, T. Nakajima, Y. Honda, O. Kitao, H. Nakai, T. Vreven, J. A. Montgomery, Jr., J. E. Peralta, F. Ogliaro, M. Bearpark, J. J. Heyd, E. Brothers, K. N. Kudin, V. N. Staroverov, T. Keith, R. Kobayashi, J. Normand, K. Raghavachari, A. Rendell, J. C. Burant, S. S. Iyengar, J. Tomasi, M. Cossi, N. Rega, J. M. Millam, M. Klene, J. E. Knox, J. B. Cross, V. Bakken, C. Adamo, J. Jaramillo, R. Gomperts, R. E. Stratmann, O. Yazyev, A. J. Austin, R. Cammi, C. Pomelli, J. W. Ochterski, R. L. Martin, K. Morokuma, V. G. Zakrzewski, G. A. Voth, P. Salvador, J. J. Dannenberg, S. Dapprich, A. D. Daniels, O. Farkas, J. B. Foresman, J. V. Ortiz, J. Cioslowski, D. J. Fox, *Gaussian 09*, Revision E.01, Wallingford CT, 2013.